VI. Conclusions

In this paper, an improved expression incorporating the skin effect for the prediction of the series resistance in a spiral inductor model has been derived. A novel modified equivalent-circuit model based on eddy-current analysis has thus been proposed. Good agreement between the simulated and measured S-parameters have been obtained.

References

[1] W. B. Kuhn and N. K. Yanduru, "Spiral inductor substrate loss modeling in silicon RFIC's," *Microwave J.*, pp. 66–81, Mar. 1999.

[2] W. B. Kuhn and N. M. Ibrahim, "Analysis of current crowding effects in multiturn spiral inductors," *IEEE J. Trans. Microwave Theory Tech.*, vol. 49, pp. 31–38, Jan. 2001.

[3] J. R. Long and M. A. Copeland, "The modeling, characterization and design of monolithic inductors for silicon RF IC's," *IEEE J. Solid-State Circuits*, vol. 32, pp. 357–369, Mar. 1997.

[4] C. P. Yue and S. S. Wong, "Physical modeling of spiral inductors on silicon," *IEEE Trans. Electron Devices*, vol. 47, pp. 560–568, Mar. 2000.

[5] A. M. Niknejad and R. G. Meyer, "Analysis, design and optimization of spiral inductors and transformers for Si RF IC's," *IEEE J. Solid-State Circuits*, vol. 33, pp. 1470–1481, Oct. 1998.

[6] R. D. Lutz, Y. Hahm, A. Weisshaar, V. K. Tripathi, A. Grzegorek, and W. McFarland, "Modeling of spiral inductors on lossy substrates for RFIC," in *IEEE MTT-S Int. Microwave Symp. Dig.*, May 1998, pp. 1855–1858.

[7] R. D. Lutz *et al.*, "Modeling of spiral inductors on lossy substrates for RFIC applications," in *Proc. RFIC Symp.*, June 1998, pp. 313–316.

[8] H.-S. Tsai, J. Lin, R. C. Frye, K. L. Tai, M. Y. Lau, D. Kossives, F. Hrycenko, and Y.-K. Chen, "Investigation of current crowding effect on spiral inductors," in *IEEE MTT-S Int. Microwave Symp. Dig.*, 1997, pp. 139–142.

[9] Y. L. Chow and I. N. Behery, "An approximate dynamic spatial Green's function for microstrip lines," *IEEE Trans. Microwave Theory Tech.*, vol. MTT-26, pp. 978–983, Dec. 1978.

Multilayer and Anisotropic Planar Compact PBG Structures for Microstrip Applications

Christophe Caloz and Tatsuo Itoh

***Abstract*—Two novel microstrip planar photonic-bandgap (PBG) structures are presented, i.e., a multilayer PBG and an anisotropic PBG. The multilayer PBG, constituted of uniplanar compact (UC) PBGs stacked up below the line, produces huge gaps (>140%) through the suppression of parasitic transmission peaks and can achieve a twofold size reduction with respect to UC-PBGs. The anisotropic PBG is a uniplanar structure exhibiting a propagation direction and an attenuation direction (AD) in a working range of the order of 35%, deep/sharp gaps broader than 65% in the AD, an excellent insensitivity to the line position and an extreme compact size of the order of $\lambda/2$ by $\lambda/7$.**

***Index Terms*—Anisotropic PBGs, monolayer/multilayer PBGs.**

I. Introduction

Recently, novel microwave photonic-bandgap (PBG) structures have been proposed [1]. Among those, the uniplanar compact photonic-bandgap (UC-PBG) structure [2], characterized by wide stopbands [3] and a slow-wave effect with very low insertion loss [4], is of particular interest because of its easy integration and low cost. Its has been demonstrated in a variety of applications including, for instance, broad-band low-pass and spurious-free bandpass filters [2] and harmonic-tuned power amplifiers [5].

In this paper, we present two novel compact planar microstrip PBG structures, which can be considered as extensions of the UC-PBG, i.e., the multilayer and anisotropic PBGs. The multilayer PBG [6] is an extension of the UC-PBG, in which several UC-PBGs, with different patterns and periods, are stacked up below the microstrip line. This structure provides additional degrees of freedom that are exploited to achieve a dramatic increase in bandwidth and reduction of size. The anisotropic PBG [7] is a uniplanar structure presenting an anisotropic geometry resulting in a propagation direction (PD) and an attenuation direction (AD). This structure also exhibits very good filtering performances in the AD with an extremely compact size.

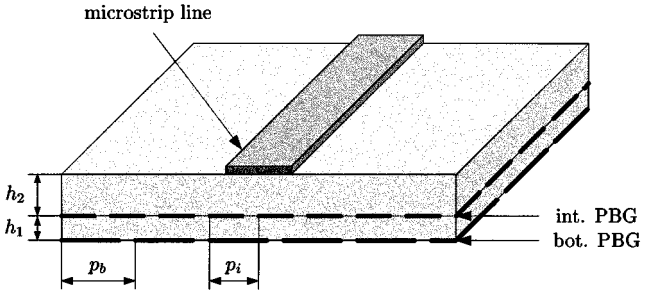

Fig. 1. Multilayer PBG architecture (bilayer case).

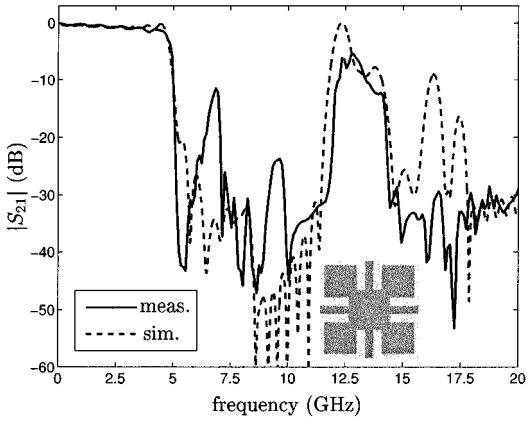

Fig. 2. Insertion loss for the monolayer PBG structure with the unit cell (a) pattern shown in the inset.

II. Multilayer PBG

The architecture of the multilayer PBG is shown in Fig. 1. We will present two variants of this structure, i.e., a harmonic configuration and an inharmonic configuration. The bottom PBG of the harmonic configuration is the conventional UC-PBG, shown in the inset of Fig. 2, and with a period $p_b = a$. The intermediate PBG (shown in the inset of Fig. 3) has the same pattern, except that the strip branches have been removed and presents a period twice smaller ($p_i = p_b/2 = a/2$). This configuration is called *harmonic* because the periods of the two PBGs are in a harmonic ratio, which results from superimposition into a structure of global period identical to the larger of the periods ($p_g = p_b = a$). Since the cutoff frequency is fixed by the larger period, it is expected to remain unchanged with respect to the case of the monolayer PBG of period a.

Manuscript received September 6, 2001.

The authors are with the Electrical Engineering Department, University of California at Los Angeles, Los Angeles, CA 90032 USA (e-mail: caloz@ee.ucla.edu).

Publisher Item Identifier 10.1109/TMTT.2002.802338.

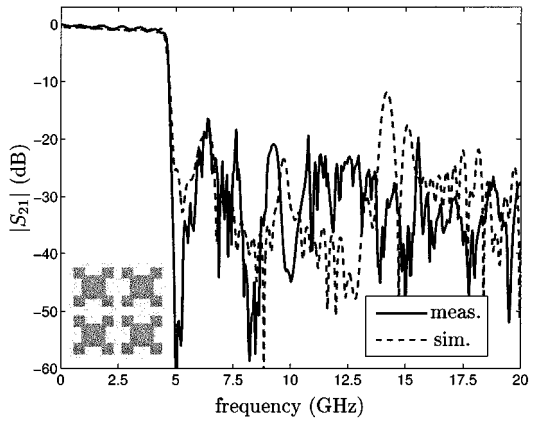

Fig. 3. Insertion loss for the bilayer harmonic PBG structure with the intermediate PBG unit cell (a) pattern shown in the inset.

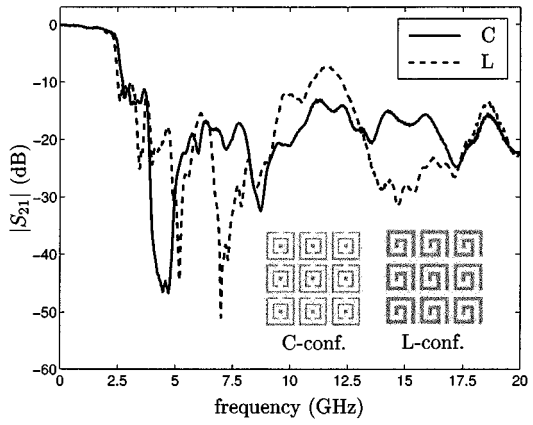

Fig. 4. Measured insertion loss for the capacitors (C) and inductors (L) configurations of the bilayer inharmonic PBG structure with the intermediate PBG unit cell ($2a$) patterns shown in the insets.

However, this configuration will be demonstrated to open up a broader bandgap from the combined effects of the two PBG layers.

In the inharmonic PBG configuration, the bottom PBG is the same as in the harmonic case, but the intermediate PBG has a period that is in an *inharmonic* ratio with that of the bottom PBG ($p_i = 2a/3$), which leads to a global period larger than the larger period ($p_g = 2a$). Consequently, a lower cutoff frequency and, therefore, a higher compactness, is expected from the inharmonic configuration, in addition to a broader bandgap. In addition, the intermediate PBG uses capacitors or inductors elements, shown in the inset of Fig. 4, which will create reactive loadings contributing to the reduction of the cutoff frequency.

The bilayer PBG of Fig. 1 is essentially a broad-band low-pass filter, in which the bottom PBG, with its larger period and dc connectivity, controls the lower frequencies, cutoff, and the first part of the gap, while the intermediate PBG, with its smaller period, controls the higher part of the gap [6]. This concept of control of adjacent frequency bands by PBGs of increasing periods can be potentially extended to a larger number of layers.

For all the structures presented in this section, the period of the bottom PBG is fixed to $a = 240$ mil and the substrates are RT/Duroid with $\varepsilon_r = 10.2$ and thicknesses of $h_1 = 10$ mil and $h_2 = 20$ mil for the lower and upper substrates, respectively. The bottom PBG contains 6×8 unit cells and the intermediate PBG then contains 12×16 and 9×12 unit cells for the harmonic and inharmonic structures, respectively.

In order to demonstrate the advantages of the bilayer PBG, we will also consider a reference monolayer PBG. The unique PBG plate of this

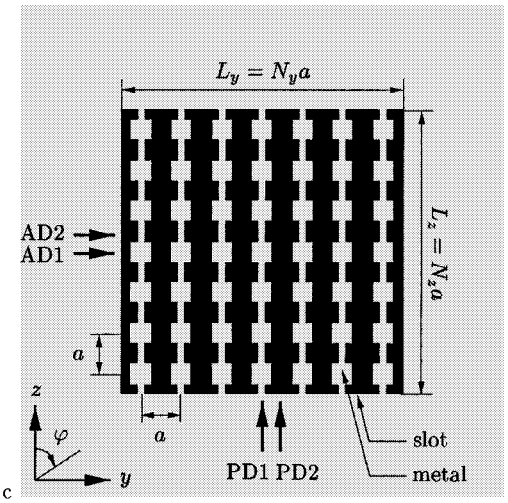

Fig. 5. Ground plane of the anisotropic PBG structure with parameters. AD and PD represent the attenuation and PDs, respectively. The darker regions represent slots.

structure is the same as the bottom PBG of the bilayer structures and its height h is such that $h = h_1 + h_2$, which means that both its transverse and normal dimensions are identical to that of the bilayer PBG.

The finite-difference time-domain (FDTD)-simulated/measured insertion loss for the reference monolayer PBG are shown in Fig. 2. The peak centered at 12.5 GHz is typical for a monolayer PBG and represents a parasitic transmission band, limiting the gapwidth here to approximately 80%.

The corresponding insertion loss for the harmonic bilayer PBG is shown in Fig. 3. The cutoff frequency ($f_c = 5$ GHz) is still, as expected, but its intermediate PBG has completely suppressed the parasitic transmission peak, thereby increasing the bandwidth of the gap from 80% to approximately 120%; in fact, to over 140%, according to measurements (not shown) up to 26.5 GHz. In addition to this huge gapwidth, we note that the insertion loss in the passband has not been increased by the introduction of the intermediate PBG. This is because the nonconnective small-period intermediate PBG is invisible to electromagnetic (EM) waves at low frequencies. Return loss, which is radiation loss in the gap, has been observed to be comparable to that of the monolayer PBG [2].

Finally, the performances of the inharmonic bilayer PBG are shown in Fig. 4. In this configuration, the cutoff frequency has been reduced by a spectacular factor of two, from 5 to 2.5 GHz. This means that, for a given desired cutoff, the transverse size of the structure has been reduced by a factor of two and corresponds to a (larger) period of $a \approx \lambda/8$, where λ is the effective wavelength in the conventional microstrip. Both observations made for the previous structure on radiation loss and passband insertion loss still hold here.

III. Anisotropic PBG

The anisotropic uniplanar PBG is a microstrip structure with a ground plane consisting of an array of etched slots of alternating widths, as shown in Fig. 5. Its pattern is a two-dimensional (2-D) square-lattice periodic structure with a unit cell geometry exhibiting a 180° symmetry. When the line is in the z-direction, the induced current can flow freely through the structure and the signal is transmitted, while the signal is rejected when the line is in the y-direction because of the stepped-impedance slots breaking the continuity of metal paths [7]. Thus, z is a PD and y is an AD.

In this structure, the period (a) is much smaller than wavelength $a \ll \lambda$, in contrast to the case of a conventional PBG, and the ground plane

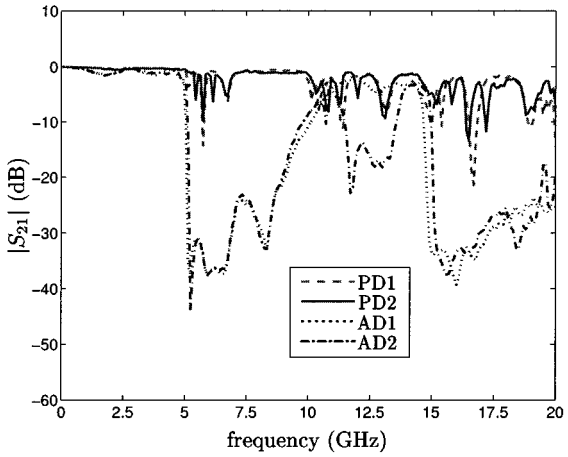

Fig. 6. Measured insertion loss for the anisotropic PBG for the line positions indicated in Fig. 5 ($N_y \times N_z = 7 \times 7$).

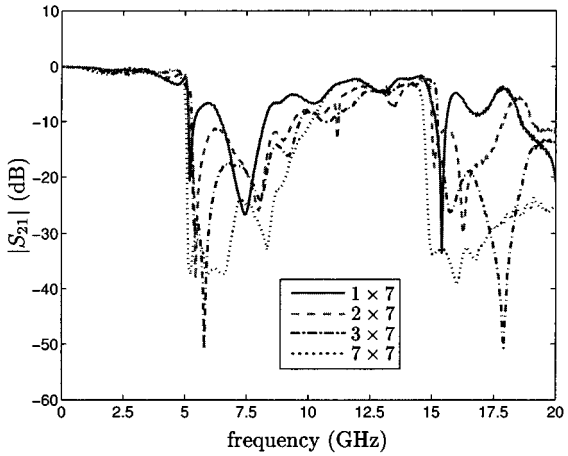

Fig. 7. Measured insertion loss of the anisotropic PBG in the AD for $N_y = 1, 2, 3, 7$ ($L_z = 7a$).

behaves, therefore, as an *effective impedance surface*. The gap (AD) is not due to Bragg-like diffraction, but to the first resonance of the array transverse stepped-impedance slots of the PBG ($L_z \approx \lambda/2$). As a direct consequence of the "impedance effectiveness," the transmission characteristics of the anisotropic PBG are essentially *insensitive to the position* of the line in both the PD and AD.

For the results presented in this section, the period is $a = 60$ mil and the substrate is RT/Duroid with $h = 25$ mil and $\varepsilon_r = 10.2$. The total dimensions of the PBG are, therefore, $L_y \times L_z = a(N_y \times N_z) = 60(N_y \times N_z)$ mil, where N_y and N_z are the number of unit cells along y and z, respectively, as shown in Fig. 5.

Fig. 6 shows the insertion loss for the different positions of the line ($a \approx \lambda/15$ at cutoff). The existence of a PD and an AD is verified in the frequency range extending from 7 to 10 GHz (35%), with a gap of 67%, which can be further increased by tapering the PBG along y. We also observe the expected excellent insensitivity to the line position in both the PD and AD. The measured return loss in the AD (not shown) varies between 0.4–3.0 dB from 5 to 10 GHz, which indicates that radiation losses of the structure are reasonable. Insertion loss in the passband could be reduced by increasing the linewidth just above the PBG, where the effective impedance is higher. A progressive evolution from the PD to the AD was observed as the angle φ of the line is increased. In addition, the structure can be easily scaled to different frequencies with $L_z = \lambda/2$. Finally, Fig. 7 shows that a small number of slots (N_y) such as two is sufficient to achieve the optimal -10-dB gap bandwidth, which leads to the extremely compact size of approximately $\lambda/2 \times \lambda/7$ ($L_z \times L_y$) in the frequency range of interest.

IV. Conclusions

Two novel planar compact PBG structures have been introduced and characterized, i.e., the multilayer PBG and uniplanar anisotropic PBG. The multilayer PBG, for which two configurations have been presented (harmonic/inharmonic), has been shown to exhibit much broader gaps (>140% versus 80%) and/or higher compactness ($2\times$ smaller) than monolayer PBGs with still very low passband insertion loss. Thanks to its compactness and super-broad-bandwidth characteristics, the bilayer PBG can be substituted for the conventional UC-PBG in several applications with enhanced performances. For instance, it can be used to reject a larger number of parasitic harmonics in bandpass filters and power amplifiers while occupying a smaller surface.

The uniplanar anisotropic PBG has a PD with excellent transmission and an PD with sharp/deep/broad bandgaps over a working range of approximately 35%, and its (first) gapwidth is larger than 65%. It is also insensitive to the position of the line on top of it, which greatly facilitates design. In addition, it can be easily scaled to other frequencies and exhibits an extremely compact size of the order of $\lambda/2 \times \lambda/7$. This structure might be introduced into applications requiring anisotropy, but also, thanks to its compactness and good gap performances, it might be used in its PD only as a low-pass or stopband filter.

References

[1] *IEEE Trans. Microwave Theory Tech. (Mini-Special Issue)*, vol. 47, Nov. 1999.

[2] F.-R. Yang, K.-P. Ma, Y. Qian, and T. Itoh, "A uniplanar compact photonic bandgap (UC-PBG) structure and its applications for microwave circuits," *IEEE Trans. Microwave Theory Tech.*, vol. 47, pp. 1509–1514, Aug. 1999.

[3] Y. Qian, F.-R. Yang, and T. Itoh, "Microstrip lines on a uniplanar compact PBG ground plane," in *Asia–Pacific Microwave Conf. Dig.*, 1998, pp. 589–592.

[4] F.-R. Yang, K.-P. Ma, Y. Qian, and T. Itoh, "A novel low-loss slow-wave microstrip structure," in *IEEE AP-S Int. Symp. Dig.*, vol. 2, Salt Lake City, UT, July 2000, pp. 1796–1799.

[5] C. Y. Hang, i V. Radisic, Y. Qian, and T. Itoh, "High efficiency power amplifier with novel PBG ground plane for harmonic tuning," in *IEEE MTT-S Int. Microwave Symp. Dig.*, vol. 2, Baltimore, MD, June 1998, pp. 807–810.

[6] C. Caloz, C.-C. Chang, Y. Qian, and T. Itoh, "A novel multilayer photonic bandgap (PBG) structure for microstrip circuits and antennas," in *IEEE AP-S Int. Symp. Dig.*, Boston, MA, May 2001, pp. 2039–2042.

[7] C. Caloz, C.-C. Chang, and T. Itoh, "A novel anisotropic uniplanar compact photonic bandgap (UC-PBG) ground plane," in *Eur. Microwave Conf. Dig.*, vol. 2, London, U.K., Sept. 2001, pp. 185–187.